Journal of Catalysis 270 (2010) 67–75

Contents lists available at ScienceDirect

Journal of Catalysis

journal homepage: www.elsevier.com/locate/jcat

Ni–Me–O mixed metal oxides for the effective oxidative dehydrogenation of ethane to ethylene – Effect of promoting metal Me

E. Heracleous [a,*], A.A. Lemonidou [a,b]

[a] Chemical Process Engineering Research Institute (CPERI), Centre for Research and Technology Hellas (CERTH), 6th km Charilaou – Thermi Road, P.O. Box 361, 57001 Thessaloniki, Greece
[b] Department of Chemical Engineering, Aristotle University of Thessaloniki, P.O. Box 1517, University Campus, 54006 Thessaloniki, Greece

ARTICLE INFO

Article history:
Received 23 October 2009
Revised 4 December 2009
Accepted 5 December 2009
Available online 4 January 2010

Keywords:
Ethane oxidative dehydrogenation
Nickel-based mixed oxides
Solid solutions
Oxygen TPD
Temperature-programmed isotopic oxygen exchange (TPIE)

ABSTRACT

This work examines the effect of Li, Mg, Al, Ga, Ti, Nb and Ta on the properties and catalytic behavior of Ni-based mixed metal oxides in the ethane oxidative dehydrogenation reaction. In all mixed oxides, with the exception of Ta, the dopants modify the NiO lattice, which contracts or expands depending on the radius of the cation, indication for the formation of solid solutions. This systematic study of doping metals varying from low (+1) to high valence (+5) elements clearly demonstrates the large effect of the dopants' valence. O_2-TPD experiments showed that increasing the valence of the foreign cation reduces the non-stoichiometric oxygen due to the cation deficient nature of the host oxide, in complete agreement with the principle of controlled valence. Temperature-programmed isotopic oxygen exchange measurements portray furthermore that not only the quantity but also the lability of the oxygen species reduces with increasing dopant valence. These electrophilic oxygen species catalyze the total oxidation reactions of ethane to CO_x, and thus their reduction/elimination favors the selective oxidation to ethylene. Ni–Nb–O exhibited the best catalytic performance with a 46% ethene yield at 400 °C, while Ni–Li–O demonstrated the worst results with a respective yield of 8.42%.

Based on the results of the present work, it can be inferred that the catalytic properties of NiO in ethane ODH can be tuned with doping, based on the nature of the dopant in Me-promoted NiO catalysts. Depending on the valence of the foreign species, the dopants can increase or decrease the unselective electrophilic oxygen radicals of NiO, leading to, respectively, reduced or enhanced ethane ODH activity.

1. Introduction

Ethylene is the keystone of the petrochemical industry. Global ethylene demand growth typically averages 4–5%/year. In 2005, global demand for ethylene increased to 107 million tons, and estimates point to ethylene supplies reaching 133 million tons by 2010 [1]. Global ethylene is produced via steam cracking of naphtha feedstocks in Europe and Asia, and ethane feedstocks in regions with associated natural gas production, including North America and the Middle East. High energy prices and relatively slow demand growth will focus ethylene producers on energy efficiency and feedstock flexibility projects, targeting to reduce the extremely high-energy demands of the endothermic steam-cracking process [2]. Moreover, stricter air quality standards proposed in the United States targeting at 90% reduction of NO_x emissions from different point sources, such as furnaces for ethylene production, will drive investments to energy-balanced, environmentally friendly ethylene production processes [2].

In this context, catalytic oxidative dehydrogenation of ethane at low temperatures is an attractive alternative route for the production of ethylene, exhibiting particular economic, technological and environmental interest [3–12]. Its major advantage, compared with the conventional method, is its high-energy efficiency, since the process operates at low temperatures and involves an exothermic reaction thus has considerably lower energy requirements. The use of ethane as feedstock greatly reduces the cost and conforms to the need for sustainable development, while the emission of greenhouse effect gases, such as NO_x and CO_2, is minimal due to the low operating temperature (<500 °C). The key for a viable industrial application of this process is the development of a highly active and selective catalytic material, able to activate and convert the relatively inert alkane to olefin at low temperature, and at the same time minimize the parallel and consecutive side reactions of both the alkane and the alkene to carbon oxides.

Ethane oxidative dehydrogenation has been studied over a wide range of catalytic materials. The most promising catalytic materials appear to be multicomponent mixed oxides. Lopez Nieto and coworkers have developed a catalytic formulation based on mixed Mo–V–Te–Nb oxides, exhibiting about 75% ethylene yield at low

* Corresponding author. Fax: +30 2310 498380.
E-mail address: eheracle@cperi.certh.gr (E. Heracleous).

0021-9517/$ - see front matter © 2009 Elsevier Inc. All rights reserved.
doi:10.1016/j.jcat.2009.12.004

reaction temperature (350–400 °C). The enhanced catalytic activity of the proposed mixed oxides was related to the presence of a multifunctional $Te_2M_{20}O_{57}$ (M = Mo, V, Nb) orthorhombic phase [8]. High ethylene yields have also been reported over chlorine-promoted non-reducible oxides (e.g. LiCl/MgO), where however the reaction proceeds at high temperature (>600 °C) via a homogeneous–heterogeneous reaction scheme [9,10].

We have recently reported [13–15] the development of highly active and selective nickel-based catalysts for the efficient dehydrogenation of ethane to ethylene in an oxidizing environment. Although the good performance of nickel-containing materials in oxidative dehydrogenation was first reported by Schuurman et al. [16], only limited research was further conducted [17–20]. The synthesis and investigation of bulk Ni–Nb–O mixed oxides by our group led to the development of low temperature, highly active and selective materials for ethane ODH that exhibit one of the best catalytic performances compared to most catalysts reported in open literature [21]. The catalyst with the optimum formulation, $Ni_{0.85}Nb_{0.15}$ catalyst, exhibits an ethylene yield of 46% at 400 °C, a yield which can compete with the efficiency of conventional naphtha steam-cracking units operating at 800 °C [14]. Detailed structural and isotopic kinetic characterization of the materials showed that due to the favorable ionic radii, valence and electron-donor properties of niobium, Nb cations fill the cationic vacancies and/or substitute nickel atoms in the NiO lattice, forming a Ni–Nb solid solution [14,15]. This substitution process is most likely responsible for the reduction of the non-stoichiometry and the cationic defects and, consequently, of the unselective oxygen species, leading to enhanced ethane ODH activity. Recently, the research group of Lopez Nieto [20] investigated alumina-supported and bulk NiO and Ni–W–O mixed oxides for the ethane ODH. Similarly to our results, the addition of tungsten was found to strongly increase the ethylene selectivity from 20% for bulk NiO to 60% for bulk Ni–W–O. XPS and Raman characterization demonstrated some interaction between NiO and WO_3 modifying the nature of Ni species, however, according to the authors, a more exhaustive study is needed to understand the possible role of tungsten in the catalytic behavior of these catalysts.

In this work, we investigate the effect of other than Nb non-reducible metals on the properties and catalytic behavior of Ni–Me–O mixed metal oxides in the ethane oxidative dehydrogenation reaction. In an effort to yield more generalized correlations, representative non-reducible metals from each periodic group (valences ranging from +1 to +5) with similar ionic radii to Ni^{2+} were selected. A series of Ni–Me–O, where Me = Li, Mg, Al, Ga, Ti and Ta, mixed metal oxide catalysts were prepared and tested in the ethane ODH. Special attention was given to the characterization of the oxygen species on the materials, investigated via advanced temperature-programmed and isotopic oxygen techniques. The effect of the doping metal on the catalytic behavior is discussed in view of the nature of the metal and the mixed oxides' physicochemical characteristics.

2. Experimental part

2.1. Catalyst preparation

A series of mixed Ni–Me–O oxides, where Me = Li, Mg, Al, Ga, Ti and Ta, with a Me/Ni atomic ratio of 0.176 was prepared by the evaporation method. In the case of Li, Mg, Al and Ga, the mixed oxides were prepared by the aqueous solutions of nickel nitrate hexahydrate (Merck) and the respective metal nitrates, lithium nitrate (Alfa-Aesar), magnesium nitrate hexahydrate (Baker), aluminum nitrate nonahydrate (Baker), gallium (III) nitrate hydrate (Sigma–Aldrich). For the preparation of the Ni–Ti–O and Ni–Ta–O samples, nickel (II) acetate tetrahydrate (Fischer) and titanium (IV) isopropoxide (Sigma–Aldrich) and tantalum (V) ethoxide (Sigma–Aldrich), respectively, in ethanol solutions were used.

In both cases, the solution containing both metals was heated at 70 °C under continuous stirring for 1 h to ensure complete dissolution and good mixing of the starting compounds. The solvent was then removed by evaporation under reduced pressure, and the resulting solids were dried overnight at 120 °C and calcined in synthetic air at 450 °C for 5 h. Pure NiO, obtained from the decomposition of nickel nitrate hexahydrate at 450 °C for 5 h in synthetic air, and Ni–Nb–O with an atomic Nb/Ni ratio of 0.176 reported by Heracleous and Lemonidou [14] were used as reference materials.

2.2. Catalyst characterization

Surface areas of the samples were determined by N_2 adsorption at 77 K, using the multipoint BET analysis method, with an Autosorb-1 Quantachrome flow apparatus. Prior to the measurements, the samples were dehydrated in vacuum at 250 °C overnight.

X-ray diffraction (XRD) patterns were obtained using a Siemens D500 diffractometer, employing Cu Kα radiation. Analysis of the XRD patterns and application of the Scherrer equation allowed the calculation of the average particle size of the samples. The lattice constant, α, of the cubic nickel oxide crystalline phase in the as synthesized mixed oxides was also determined from the obtained diffractograms.

UV–vis spectra were recorded in the 11,000–50,000 cm^{-1} range on a HITACHI U-3010 UV/vis spectrophotometer. The measurements were performed in ambient atmosphere with a scanning speed of 60 nm/min. Fused silica was used as white reference.

The reduction characteristics of the catalysts were studied by temperature-programmed reduction (TPR) experiments performed in a gas flow system equipped with a quadrupole mass analyzer (Omnistar, Balzers). Typically, the catalyst sample (50 mg) was placed in a U-shaped quartz reactor and pretreated in flowing He for 0.5 h at 450 °C, followed by cooling at room temperature. The temperature was then raised from room temperature to 800 °C with a heating rate of 10 °C/min in a 5% H_2/He flow (50 cm^3/min). The main (m/z) fragments registered were H_2 = 2, H_2O = 18 and He = 4.

The oxygen desorption properties of selected catalysts were studied by O_2-TPD measurements. The catalyst sample (200 mg) was pretreated in a flow of pure oxygen at 450 °C for 1 h and cooled to room temperature under the oxygen flow. The system was subsequently flushed with helium for 1 h, and the temperature was raised to 850 °C at a heating rate of 15 °C/min in He (50 cm^3/min). The reactor exit was monitored online by a quadrupole mass analyzer (Omnistar, Balzers), and the desorbed oxygen was detected by following the 32 (m/z) fragment. Calibration of the mass analyzer was performed with O_2/He mixtures of known concentration. Quantitative estimation of the amount of desorbed oxygen was performed by integration of the corresponding oxygen desorption rates with time.

Temperature-programmed isotopic oxygen exchange experiments (TPIE) were also performed in the earlier mentioned apparatus. Before each experiment, the catalyst (25 mg) was pretreated in 10% $^{16}O_2$/He flow at 450 °C for 1 h, followed by flushing in He for 1 h and subsequent cooling to room temperature. The catalyst sample (250 mg) was subjected to 2% $^{18}O_2$ (Cambridge Isotope Laboratories; 95% atom enrichment)/He flow (40 cm^3/min), and the temperature was raised from room temperature to 650 °C at a heating rate of 15 °C/min. The system was maintained isothermally at 650 °C for 30 min under the reactant mixture. The reactor exit was connected by a heated inlet capillary system to a quadrupole mass analyzer (Omnistar, Balzer) for the online monitoring of the

exit gas composition. The concentration profiles were obtained by registering the following (m/z) fragments: He = 4, H_2O = 18, N_2 = 28, $^{16}O_2$ = 32, $^{16}O^{18}O$ = 34 and $^{18}O_2$=36. Calibration of the mass analyzer was performed with O_2/He mixtures of known concentration. The total amount of exchangeable ^{16}O species in each catalyst was calculated from the integration of the corresponding TPIE ^{16}O surface formation rate, expressed as the sum of ^{16}O in $^{16}O^{18}O$ and $^{16}O_2$ surface formation rates, with time. The apparent activation energy of the exchange reaction was calculated from Arrhenius plots for the $^{18}O_2$ surface consumption rate. The data points used for the construction of the Arrhenius plots corresponded to $^{18}O_2$ conversions lower than 10%, in order to maintain the assumption of differential conditions in the reactor valid.

2.3. Reactivity studies

The catalytic performance of the samples was measured in a fixed-bed quartz reactor. The catalyst particles were diluted with equal amount of quartz particles of the same size to achieve isothermal operation. The temperature in the middle of the catalytic bed was measured with a coaxial thermocouple. The samples were activated in flowing oxygen at 450 °C for 30 min. The composition of the reaction mixture used was 9.1%C_2H_6/9.1%O_2/81.8%He.

The oxidative dehydrogenation of ethane was investigated in the temperature range from 300 °C to 425 °C. For the determination of the activity of the catalysts as a function of temperature, the W/F ratio was kept constant at 0.54 g s/cm^3. In order to obtain different ethane conversion levels at constant reaction temperature (400 °C), the W/F ratio was varied from 0.02 to 0.71 g s/cm^3.

The reaction products were analyzed online by a Perkin–Elmer gas chromatograph equipped with a thermal conductivity detector (TCD). Two columns in a series-bypass configuration were used in the analysis: a Porapak Q and a MS 5A. The main reaction products were C_2H_4, CO_2 and H_2O. Negligible amounts of oxygenates were observed at the reactor exit. The ethane conversion and the selectivity to the reaction products were calculated on a carbon basis. Closure of the carbon mass-balance was better than ±1%. The contribution of gas-phase initiated reactions was tested by conducting experiments using an empty-volume reactor. The conversion of ethane at these experiments was lower than 1%, confirming that gas-phase reactions are negligible at the experimental conditions used for the activity tests.

3. Results and discussion

3.1. Catalyst characterization

The main physicochemical characteristics of the Ni–Me–O mixed oxides are tabulated in Table 1. The surface areas of the mixed oxides vary considerably depending on the promoting metal, with relatively large surface areas recorded for Ni–Nb–O, Ni–Al–O, Ni–Ga–O and Ni–Ta–O. The mixed oxides of Li, Mg and Ti yielded similar surface areas as pure NiO.

X-ray diffraction (XRD) was employed for investigating the crystalline phases formed in the calcined catalysts. Fig. 1 illustrates the diffractograms obtained for all the samples plus that of NiO and Ni–Nb–O used as reference. In most Ni–Me–O mixed oxides, XRD analysis exhibits only diffraction lines corresponding to a crystalline "NiO-like" phase. In the Ni–Nb–O sample, the appearance of an additional broad band centered at 2θ 27° is apparent. This diffraction has been attributed to an amorphous niobium-rich phase [14,22]. In Ni–Ti–O, minor amounts of free TiO_2 anatase are also formed, evidenced by the diffractions at 2θ 27°, 48° and 54°, while for Ni–Ta–O, very poor crystallization is generally observed with diffraction lines corresponding to NiO and $NiTa_2O_6$ at 2θ 26.7°, 35° and 53°.

The XRD patterns were also used to estimate the average particle size of NiO in the as synthesized materials using the Scherrer equation. The results shown in Table 1 evidence that all Ni–Me–O mixed oxides consist of NiO crystallites in the nanorange, with sizes ranging from 17 nm for the Ni–Nb–O catalyst to 40 nm for the Ni–Ta–O sample.

Further analysis of the XRD patterns allowed the calculation of the lattice parameters of the nickel oxide-like phase in the as synthesized mixed oxides, presented in Table 1. The XRD analysis shows that pure NiO crystallizes in the cubic rock salt structure with a lattice constant of a = 4.1762 Å, in agreement with reported data (JCPDS 4-835). The changes observed in the size of the NiO unit cell in the mixed oxides indicate the incorporation of the dopants in the NiO structure and the formation of Ni–Me–O solid solutions. The graphic depiction of the NiO-like phase lattice constant as a function of the difference in ionic radii between Ni^{2+} and doping ion clearly confirms the above. As seen in Fig. 2, the NiO unit cell size expands or contracts according to the radius of the foreign cation in comparison with that of the host (Ni^{2+}). This supports our previous findings on the Ni–Nb–O system [14], according to which niobium species (Nb^{5+}) substitute some of the host cations (Ni^{2+}) and/or fill in cationic vacancies in the NiO structure leading to the formation of a nickel–niobium solid solution and subsequently to a contraction of the NiO lattice, since the radii of Nb^{5+} is smaller than that of Ni^{2+}.

It can be therefore deduced that in Ni–Me–O mixed oxides, dopants can insert the NiO lattice relatively easy and form solid solutions, independent of the valence of the foreign species which ranged in our study from +1 to +5. What seems to be important is the ionic radius of the dopants – the main criterion for the selection of the investigated doping elements – which has to be similar to Ni^{2+}.

UV–vis spectroscopy was applied in order to study the coordination of the nickel species in the Ni–Me–O mixed metal oxides. The UV–vis spectra are presented in Fig. 3. It should be mentioned that high absorbance was recorded over the whole measured wavelength range because of the dark (gray) color of the samples, indicating the presence of nickel in a non-stoichiometric form and resulting in weak absorbance bands. Moreover, the Ni–Li–O sample did not give rise to any bands due to its extremely dark color and is

Table 1
Nomenclature and physicochemical characteristics of the catalysts.

Catalyst	Valence of Me	Me ionic radius (Å)	Surface area (m^2/g)	NiO average crystal size (nm)	NiO lattice constant (Å)	Desorbed O_2 (mg/g)
NiO	–	0.69	16.7	31.8	4.1762	4.9
Ni–Nb	+5	0.64	85.1	16.7	4.1725	0.6
Ni–Li	+1	0.60	7.6	28.0	4.1704	5.9
Ni–Mg	+2	0.86	19.2	29.9	4.1847	4.0
Ni–Al	+3	0.67	67.8	32.3	4.1781	2.1
Ni–Ga	+3	0.76	45.3	27.3	4.1805	2.3
Ni–Ti	+4	0.61	18.6	22.7	4.1750	0.05
Ni–Ta	+5	0.78	78.9	40.2	4.1785	0.4

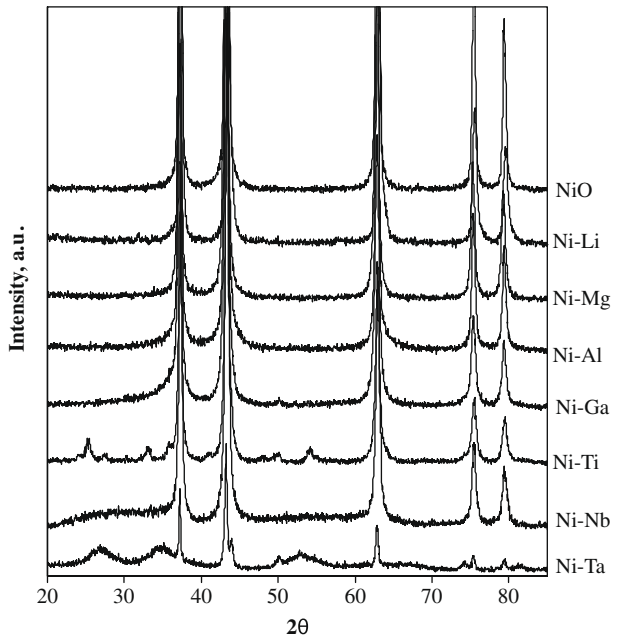

Fig. 1. X-ray diffraction patterns of the Ni–Me–O catalysts and NiO reference material.

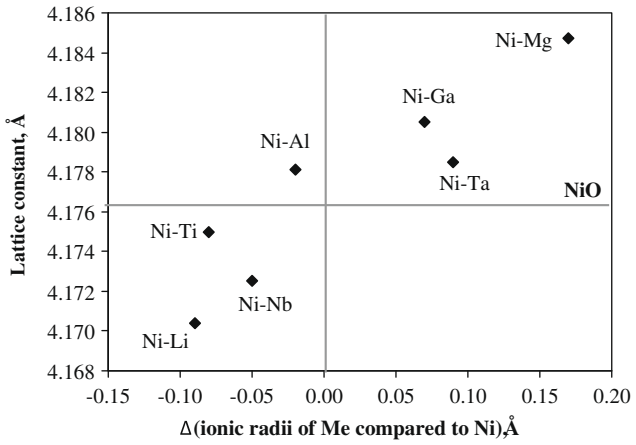

Fig. 2. Lattice constant, α, of the NiO-like phase in the Ni–Me–O catalysts as a function of the difference in ionic radii between Ni^{2+} and dopant ion Me^{x+}.

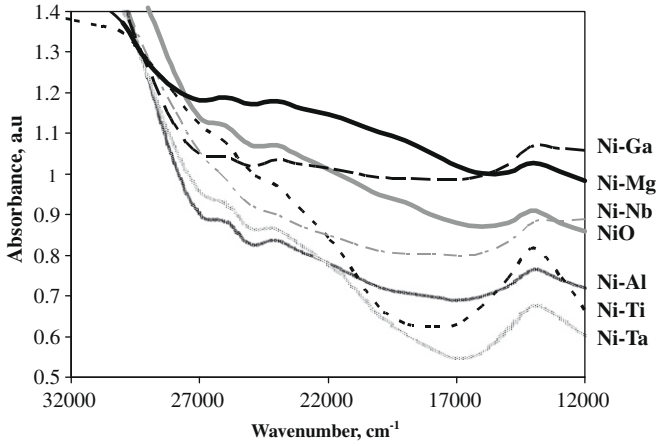

Fig. 3. UV–vis spectra of the Ni–Me–O catalysts and NiO reference material.

therefore not included in the figure. NiO has a rock salt structure with Ni ions in an octahedral coordination. The NiO spectrum is dominated by absorption bands in the 16,500–11,000 cm^{-1} range, due to the d–d transitions of octahedral Ni(II) in the NiO lattice. The band at 26,500 cm^{-1} and the strong band at 14,000 cm^{-1}, ascribed to the $^3A_{2g} \rightarrow {}^3T_{1g}(F)$ transition of octahedral Ni(II), are fingerprints for NiO [23]. The spectra acquired for the Ni–Me–O mixed oxides closely resemble that of NiO with main bands at 14,000 and 26,500 cm^{-1} indicating, in accordance with the XRD results, that the NiO structure is pertained in the mixed oxides with Ni(II) in octahedral coordination. This result supports the general notion that the dopants are incorporated in the NiO structure, and Ni–Me–O solid solutions are formed.

Temperature-programmed reduction in H_2 was performed in order to study the reduction characteristics of the as synthesized nickel-based mixed oxide catalysts. The TPR profiles, shown in Fig. 4, were acquired by continuously following the H_2 signal with a quadrupole mass spectrometer, while linearly increasing temperature. The TPR profiles of the reference materials NiO and Ni–Nb–O are also included for comparison reasons in Fig. 4. NiO exhibits a narrow reduction peak with a maximum at 415 °C, with the amount of consumed hydrogen corresponding to total reduction to metallic Ni. The introduction of Nb causes the appearance of a high temperature shoulder and broadens the reduction profile, while shifting the reduction temperature of the main peak to ~360 °C. According to our previous results [14], the main peak is attributed to the reduction of Ni–O–Ni bonds and the broad shoulder to the removal of oxygen from Ni–O–Nb bonds.

The introduction of other than Nb metals also significantly modifies the reduction profiles, as shown in Fig 4. While Nb was found to ease the reduction of Ni–O–Ni bonds, shifting the reduction temperature at lower values, all other metals seem to inhibit the reduction process compared to pure NiO. Ni–Li–O and Ni–Al–O exhibit similar profiles to NiO with one main reduction peak, shifted to +10 °C and +35 °C higher temperature, respectively. Ni–Ti–O and Ni–Ga–O on the other hand display three peaks, indicating the contribution of three different distinct species in the reduction process. In both cases, the main reduction temperature

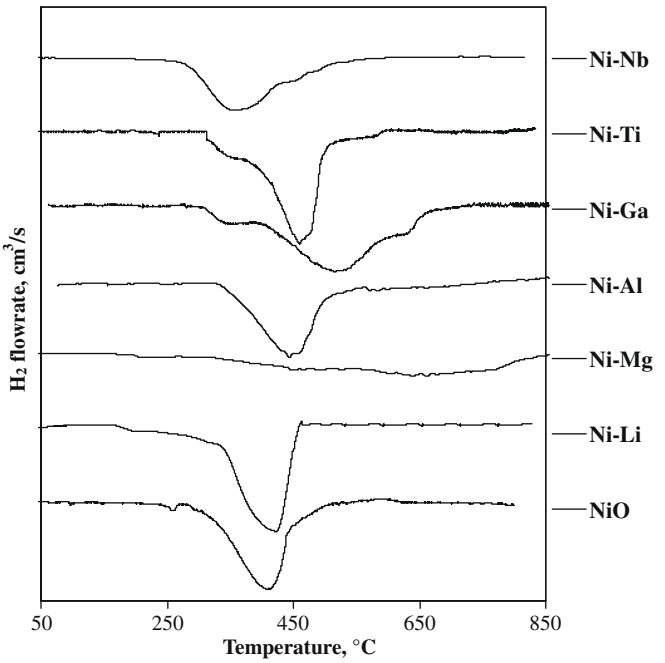

Fig. 4. Temperature-programmed reduction profiles of the Ni–Me–O catalysts and NiO reference material.

is again shifted to higher temperatures, 470 °C and 530 °C for Ti and Ga, respectively. Finally, the mixed oxide with Mg shows a very low reducibility with a broad peak at very high temperature >650 °C. This result agrees with previous TPR-H_2 studies [24,25], which attributed the very low reducibility of Ni–Mg–O mixed oxide to the formation of non-reducible spinel precursors in a very early stage (not detectable by XRD).

Besides the reduction temperature, the presence of the promoters also modifies the consumption of hydrogen in the TPR experiments. It is interesting to comment on the ratio of hydrogen consumption versus the stoichiometrically required hydrogen to completely reduce the nickel species present in the Ni–Me–O mixed oxides. A ratio of 1 was calculated for the Ni–Li–O, Ni–Ti–O, Ni–Nb–O and NiO samples, indicating that the recorded reduction curves can be attributed only to the complete reduction of Ni^{2+} cations to metallic nickel. Ni–Ga–O on the other hand exhibits a ratio higher than 1, showing that besides the full reduction of nickel species, gallium cations also undergo a full reduction from +3 to 0. Ni–Mg–O and Ni–Al–O are the only two materials with a lower H_2 consumption than that required for the full reduction of the nickel species. In accordance with the above, this can be attributed to the presence of non-reducible, spinel-like phase precursors in these two mixed oxides.

Pure NiO, calcined at low temperatures, is a well-known non-stoichiometric oxide with cationic deficiency. This property renders NiO a good p-type semiconductor with its conductivity being attributed to this cation deficiency [26,27]. The cationic vacancies induce the formation of positive holes p+, the main charge carriers, which are introduced in the form of Ni^{3+} or O^- ions to keep charge neutrality conditions [28,29]. Our previous electrical conductivity and O_2 desorption (TPD) studies on NiO [14] validated the above, as NiO was found to accommodate a large amount of non-stoichiometric oxygen and demonstrated a large oxygen desorption peak in the 450–850 °C temperature range, in agreement with O_2-TPD measurements on NiO reported in literature [17]. Moreover, investigations on Ni–Nb–O mixed oxides [14] showed that the dissolution of a higher valence cation, such as Nb^{5+}, in the p-type cation deficient NiO lattice reduces the positive hole p^+ concentration and, consequently, the non-stoichiometric oxygen. From the electrical point of view, the dissolution of hetero-valent ions in the lattice of a host oxide creates free charge carriers (electrons or holes) in order to maintain electrical neutrality. It is therefore expected that the dissolution of lower valence cations should have the opposite effect, i.e. charge compensation should occur by additional formation of O^- species and consequently increase in the non-stoichiometric oxygen. To verify this hypothesis, we performed O_2-TPD measurements on the synthesized Ni–Me–O mixed oxides. The profiles of oxygen desorption with increasing temperature are compiled in Fig. 5 for all Ni–Me–O oxides, plus that of reference NiO and Ni–Nb–O. The amount of oxygen desorbed, expressed in mg O_2 per gram of catalyst, is tabulated in Table 1. Indeed, the oxygen desorption profiles change dramatically in the mixed oxides compared to pure NiO. The incorporation of Li^{1+} in NiO results in a second oxygen species desorbed at significantly lower temperature (~380 °C compared to ~700 °C for pure NiO), indicating the formation of a second very active form of oxygen. It is also important to note that Ni–Li–O is the only material that desorbs a higher amount of oxygen than NiO, in complete agreement with theory, since Li is the only cation with lower valence than Ni. Our results are in line with the work of El-shobaky and Petro [30], who studied the effects of Li-doping on the electrical properties and surface characteristics of NiO and found that Li-doping considerably increased the non-stoichiometric oxygen of NiO (determined iodometrically), as well as its electrical conductivity. In Ni–Mg–O, the second oxygen species observed on Ni–Li–O at 380 °C is reduced to a shoulder with a broader main desorption peak located at the same temperature as in NiO, ~700 °C. The amount of oxygen desorbed is similar to NiO, an anticipated result given the fact that complete solid solubility exists between the two systems as both components are cubic oxides of equal valence [31].

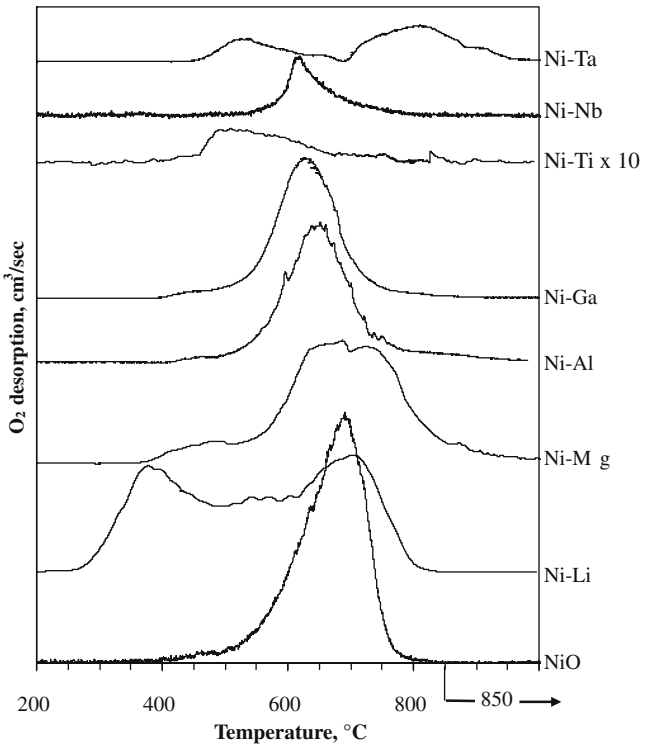

Fig. 5. Temperature-programmed oxygen desorption curves of Ni–Me–O catalysts and NiO reference material.

As the valence of the doping metals increases from +3 to +5, a progressive reduction in the amount of desorbed oxygen is recorded, while a shift in the temperature of desorption is also observed. For Ni–Al–O, Ni–Ga–O, Ni–Ti–O and Ni–Nb–O, only one main desorption peak is observed with maximum desorption temperature at 655 °C, 635 °C, 500 °C and 625 °C, respectively. In the case of Ni–Ta–O, two small peaks are again detected at 530 °C and 820 °C which can be possibly attributed to oxygen desorption from the $NiTa_2O_6$ and the NiO phase, respectively. It is reminded that Ni–Ta–O was the only mixed oxide with very poor crystallization and not clearly identifiable structure.

Overall, the oxygen TPD-O_2 experiments clearly support and confirm the notion that the doping metals insert the NiO lattice and successfully form Ni–Me–O solid solutions. The quantitative results are consistent with the principle of controlled valence [32], since the dissolution of lower than nickel valence cations (Li^{1+}) increases the non-stoichiometric oxygen in NiO, while the higher valence cations (Al^{3+}, Ga^{3+}, Ti^{4+} Nb^{5+}, Ta^{5+}) act as electron donors and reduce the positive p^+ hole concentration and consequently the electrophilic O^- radicals of the NiO acceptor. It should be noted that the repetition of the O_2-TPD experiments without prior O_2 adsorption yielded the same desorption patterns. This indicates that the desorbed oxygen originates from the bulk structure of the materials under study.

Finally, temperature-programmed $^{18}O_2$ isotope exchange measurements were conducted in order to obtain further insight on the oxygen species and the type and density of sites available for oxygen activation on the Ni–Me–O mixed oxides. The temperature-programmed isotope oxygen exchange profiles in the 30–650 °C temperature range for all Ni–Me–O oxides, plus that of reference NiO and Ni–Nb–O, are shown in Fig. 6, where the surface

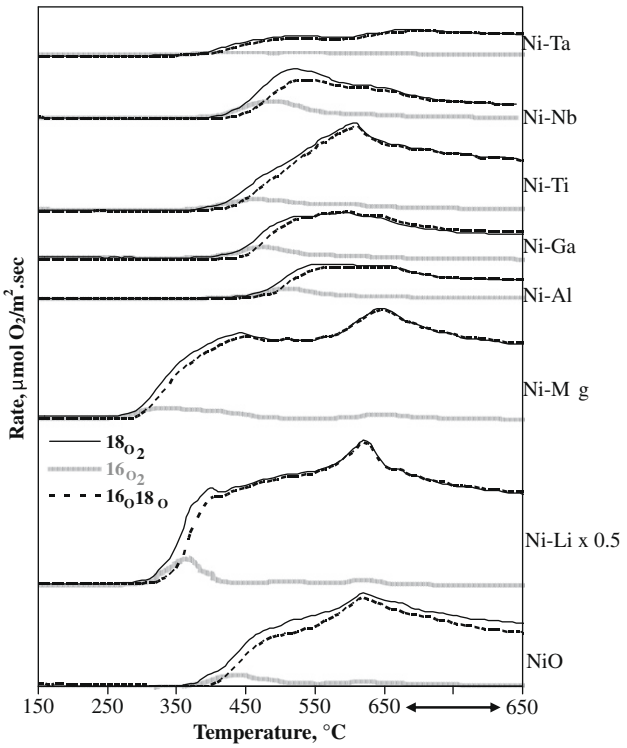

Fig. 6. Temperature-programmed $^{18}O_2$ isotopic oxygen exchange profiles of Ni–Me–O catalysts and NiO reference material.

consumption and formation rate of all isotopic species ($^{18}O_2$, $^{16}O^{18}O$ and $^{16}O_2$ species) is depicted as a function of temperature. The oxygen balance in all experiments amounted to 95±5% and hence, the amount of oxygen consumed for any irreversible adsorption or desorption was not significant. A first general observation concerning the TPIE profiles is that the exchange process occurs on all materials via both the simple (R1 mechanism – exchange of only one surface oxygen species) and the multiple (R2 mechanism – simultaneous exchange of two surface oxygen species) heteromolecular ^{18}O isotope exchange mechanism [33,34]. Moreover, on all materials, the exchange takes place initially via the multiple exchange mechanism, since the first product detected is $^{16}O_2$, and then proceeds, as the surface is depleted of ^{16}O, via the dominant simple exchange mechanism, leading to the formation of $^{16}O^{18}O$ cross-labeled species. It can be also observed that the oxygen exchange process commences at low temperature on all solids, temperature range of interest for the actual catalytic reaction. It should be commented here that the onset temperature for the oxygen exchange is slightly higher than the temperature where oxidative dehydrogenation occurs on the Ni–Me–O oxides. Based on our previous experience with isotopic experiments under oxidizing and reaction atmosphere [15], we postulate that when the surface is partially reduced, oxygen vacancies are created, and thus lattice oxygen mobility is enhanced compared to exchange in the absence of the alkane, thus explaining the observed temperature difference.

The introduction of dopants in the NiO structure modifies, as in the case of the O_2-TPD experiments, both the quantity and mobility of the exchanged oxygen species. The exchange curves of all materials demonstrate the existence of at least two types of exchangeable oxygen species, one active in the 350–550 °C temperature range and a second one mobile at higher temperatures >550 °C. Although both species exist on all catalysts, their quantity and proportion vary with the different dopants. As the valence of the dopant increases, the oxygen mobile at higher temperatures seems to reduce. The Ni–Ti–O and Ni–Ta–O catalysts constitute an exception to the above, as the amount of high-temperature oxygen species seems to be quite high although Ti and Ta have a valence of +4 and +5, respectively.

Table 2
Quantitative results of the temperature-programmed $^{18}O_2$ isotopic oxygen (TPIE) experiments.

Catalyst	Valence of Me	Total μmol of ^{16}O atoms exchanged/m^2	E_a (kJ/mol)
NiO	–	264	114.6 ± 0.5
Ni–Nb	+5	120	175.6 ± 0.7
Ni–Li	+1	637	24.6 ± 0.3
Ni–Mg	+2	424	105.8 ± 0.9
Ni–Al	+3	92	175.2 ± 3.6
Ni–Ga	+3	224	138.2 ± 2.9
Ni–Ti	+4	238	138.3 ± 2.0
Ni–Ta	+5	90	137.8 ± 1.6

Quantitative results of the temperature-programmed $^{18}O_2$ isotopic oxygen (TPIE) experiments are shown in Table 2. Indeed, the total amount of the oxides' exchangeable oxygen species (estimated from the integration of the TPIE ^{16}O response curves, expressed as the sum of ^{16}O in $^{16}O^{18}O$ and $^{16}O_2$) depends greatly on the valence of the doping metal. The introduction of Li and Mg, with valence lower and equal to that of Ni^{2+}, greatly increases nickel oxide's exchangeable oxygen, while the higher valence cations (Al^{3+}, Ga^{3+}, Ti^{4+} Nb^{5+}, Ta^{5+}) have the opposite effect and reduce the catalysts' ^{16}O species available for exchange.

As aforementioned, not only the quantity but also the lability of the oxygen species changes in the presence of the different dopants. The temperature dependence of the conversion of $^{18}O_2$ to the various oxygen isotopes allowed the estimation of the apparent activation energy of the exchange reaction for the Ni–Me–O mixed oxides (see Table 2). The value of 114.6 kJ/mol for NiO is in good agreement with results reported by Winter [34]. The introduction of the dopants with valences ranging from +1 to +5 affects, in the same pattern observed with all previous results, also the activation energy for the exchange: Li and Mg, with valence lower and equal to that of Ni^{2+}, decrease the activation energy compared to NiO, while the higher valence cations (Al^{3+}, Ga^{3+}, Ti^{4+} Nb^{5+}, Ta^{5+}) have the opposite effect and progressively increase it. Therefore, it can be safely stated that the introduction of high valence dopants in NiO results in fewer and more strongly bonded oxygen species available for exchange, and consequently, for participation in the catalyst reaction.

3.2. Catalytic performance in ethane ODH

The activity of the Ni–Me–O mixed oxide catalysts in the ethane oxidative dehydrogenation reaction was explored under steady state conditions between 300 and 450 °C with a constant W/F (0.54 g s/cm^3) and ethane-to-oxygen (1/1) ratio. It should be noted that in all cases, oxygen conversion did not exceed 90%. It is also important to mention that ethylene and carbon dioxide were the only products detected in almost all catalysts, with the exception of Ni–Mg–O, Ni–Ga–O and Ni–Ti–O where minor amounts of CO (maximum selectivity <4%) were also recorded. Therefore, main reactions taking place over nickel-based catalysts are the primary selective oxidative dehydrogenation of ethane to ethylene, the primary unselective total oxidation of ethane to CO_2 and the secondary overoxidation of the produced olefin to CO_2. The presence of only CO_2 as by-product is a major advantage and renders these materials very attractive from an engineering point of view since the separation costs downstream the reactor would be greatly reduced in a potential industrial application of an oxidative dehydrogenation process.

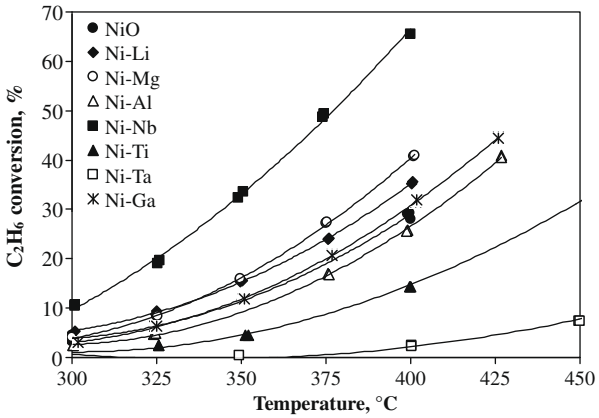

Fig. 7. Ethane conversion as a function of temperature (reaction conditions: $W/F = 0.54$ g s cm^{-3}, $C_2H_6/O_2 = 1/1$).

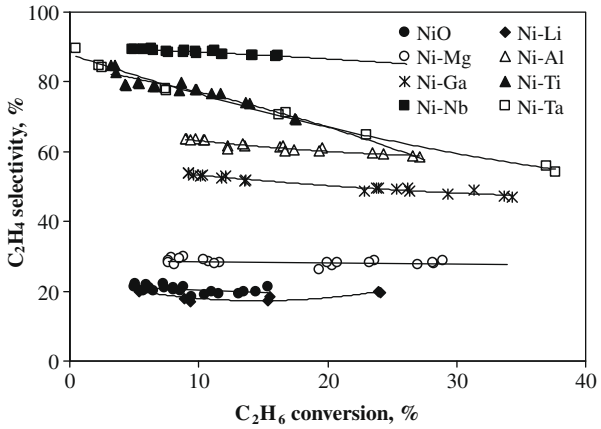

Fig. 8. Ethene selectivity as a function of ethane conversion (reaction conditions: $T = 400$ °C, $C_2H_6/O_2 = 1/1$).

Ethane conversion is plotted as a function of temperature in Fig. 7. Wide variations can be observed in the activity of the nickel-based mixed oxides based on the dopant, with ethane conversion ranging from ~2% for Ni–Ti–O to ~66% for Ni–Nb–O at 400 °C. Our previous investigations [14] on the Ni–Nb–O system revealed that surface-exposed nickel sites constitute the active centers for the activation of the paraffinic substrate. It is therefore evident that the nature of the promoting metal drastically affects the properties and the ability of the nickel sites to activate ethane at low temperature. Ni–Nb–O exhibits the highest ethane conversion, while the reactivity of the rest of the catalysts roughly inversely follows the valence of the dopants in the following order: Ni–Nb ≫ Ni–Mg > Ni–Li > Ni–Ga = NiO ⩾ Ni–Al ≫ Ni–Ti ≫ Ni–Ta.

To account for the different surface areas of the samples, the activity of the catalysts in terms of specific surface activity (SSAc) – expressed as μmol C_2H_6 consumed/m^2 s – was also considered. Based on this definition, the reactivity of the tested catalytic materials at 350 °C decreases as follows (SSAc at 350 °C shown in brackets): Ni–Li (0.139) ≫ Ni–Mg (0.055) ≈ NiO (0.049) > Ni–Nb (0.028) > Ni–Ga (0.018) = Ni–Ti (0.017) ⩾ Ni–Al (0.011) ≫ Ni–Ta (0.0004). The Ni–Li–O oxide exhibits now by far the highest surface reactivity for ethane activation, due to its very small surface area which thus increases the surface activity. However, as will be shown in the next paragraph, ethane activation on Ni–Li–O is highly unselective leading to combustion and will be further commented in the discussion. The reactivity order for the rest of the Ni–Me–O oxides under study does not change dramatically when compared on a surface activity basis.

The most important requirement for a good ODH catalyst is the ability to effectively convert ethane to ethylene at low temperature with a high selectivity. In order to study the selectivity of the mixed Ni–Me–O oxides and since selectivity is generally strongly related to conversion, we conducted a second series of experiments at constant temperature (400 °C), constant ethane/oxygen ratio (1/1) and varying W/F from 0.02 to 0.71 g s cm^{-3} to attain different conversion levels. Ethylene selectivity as a function of ethane conversion is presented in Fig. 8. The corresponding data for the NiO and Ni–Nb–O reference materials in Fig 8, taken from [14], were obtained at 350 °C. Again, significant differences can be observed between the different mixed nickel oxides depending on the nature of the promoting metal. The data clearly demonstrate that the higher the dopant cation's valence, the higher the initial selectivity to the desired product, with Ni–Nb exhibiting the highest selectivity (90%) and Ni–Li the lowest (19%). Over most Ni–Me–O catalysts, ethylene selectivity remains fairly constant with increasing ethane conversion. The secondary overoxidation of the produced alkene, which causes the drop of selectivity with increasing conversion, constitutes the main problem of ODH catalysts. These materials exhibit very stable ethene selectivity, indicating that they are reactive toward ethane but have a very low affinity to ethylene, thus preserving the olefin from further oxidation. Exceptions constitute the Ni–Ti–O and Ni–Ta–O materials where a clear decay of the selectivity to ethylene is observed with increasing ethane conversion. It is of interest to remark that these two catalysts were the only mixed oxides that demonstrated a similar in shape oxygen desorption peak at ~500 °C. Moreover, whereas increasing dopant valence was found to decrease the amount of oxygen species exchanged at high temperature in the temperature-programmed isotopic oxygen exchange experiments, Ni–Ti–O and Ni–Ta–O were again the only exceptions in this trend and exhibited a relatively large peak corresponding to these species. It could be thus inferred that the increased affinity of the Ti- and Ta-doped NiO to ethylene could be attributed to this high-temperature oxygen species; however, further investigations are needed in order to shed light into the nature and reactivity of the different oxygen species on the catalysts.

Furthermore, the TPIE results showed that the dopants influence not only the amount but also the mobility of the oxygen species present in the catalytic oxides. Li and Mg, with valence lower/equal to that of Ni^{2+}, were found to increase the lability of the oxygen species compared to pure NiO, while the presence of higher valence cations (Al^{3+}, Ga^{3+}, Ti^{4+} Nb^{5+}, Ta^{5+}) resulted in more strongly bonded oxygen groups. Our previous work on the NiO and Ni–Nb–O system [15] revealed a correlation between the ability of the catalysts to convert ethane and exchange oxygen. When the same correlation was attempted with the data of the present study, using dopants with different valences, a clear relationship between the surface rate of ^{16}O exchange at 450 °C in the TPIE experiments and the surface rate of C_2H_6 consumption at 375 °C in the activity tests was demonstrated for all catalysts, with the exception of Ni–Ta–O (see Fig. 9). The comparison of the two rates was performed at different temperatures, as previous isothermal isotopic oxygen exchange experiments on NiO and Ni–Nb–O under oxidizing and under reaction conditions [15] demonstrated clearly that in the presence of both oxygen and ethane in the feed, oxygen mobility is significantly higher than under purely oxidizing conditions. When the surface is partially reduced, due to the presence of reductive ethane, oxygen vacancies are created, and lattice oxygen mobility is enhanced compared to exchange in the absence of the alkane. Therefore and in order to correctly correlate the mobility of oxygen species truly involved in the reaction, a surface rate of oxygen exchange at higher temperature than the surface rate of ethane consumption in activity tests was chosen. The established

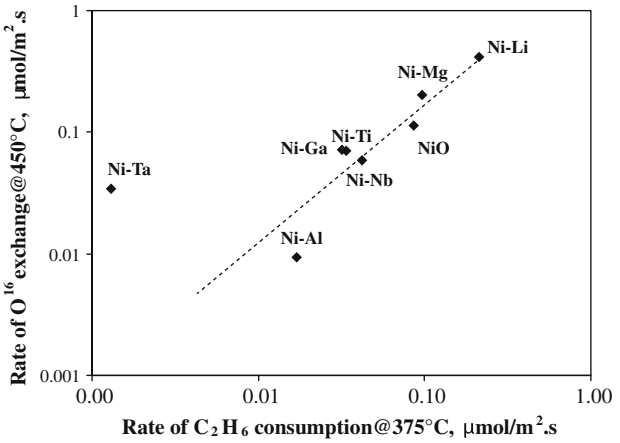

Fig. 9. Surface rate of ^{16}O exchange at 450 °C (TPIE experiments) versus surface rate of ethane conversion at 375 °C (ODH experiments).

correlation between the two rates confirms that the oxygen species exchanged in the TPIE experiments do participate and play an active role in the mechanism of ethane activation and conversion, and their amount can be tuned with dopants of different nature and valence in Me-promoted NiO catalysts.

Finally, a clear correlation between the non-stoichiometric oxygen that catalysts accommodate and the ability to selectively convert the ethane substrate to ethylene was established. In Fig. 10, ethylene selectivity at 10% ethane conversion and the amount of non-stoichiometric oxygen, derived from the TPD-O_2 experiments, are plotted for each Ni–Me–O oxide as a function of the foreign cation valence. It is clearly portrayed that these two values follow an inverse trend with increasing foreign cation valence, i.e. with increasing valence, the non-stoichiometric oxygen of the oxide is reduced and selectivity is increased. The non-stoichiometric oxygen accommodated in the Ni-based catalysts has been also previously reported to inversely correlate with the selectivity to ethylene [17,35]. Xu et al. [35] investigated the ethane ODH catalytic behavior of NiO pretreated in oxygen at 500 °C and 700 °C and found that the amount of non-stoichiometric oxygen can be controlled by the pretreatment temperature. In agreement with the present results, the authors observed that the selective activity toward ethylene decreases with the increasing amount of non-stoichiometric oxygen species in NiO. The increase in ethylene selectivity with increasing dopant valence in the Ni–Me–O mixed oxides can also be related to the less mobile oxygen species of high valence doped NiO, which appear to be more selective and convert ethane to ethylene.

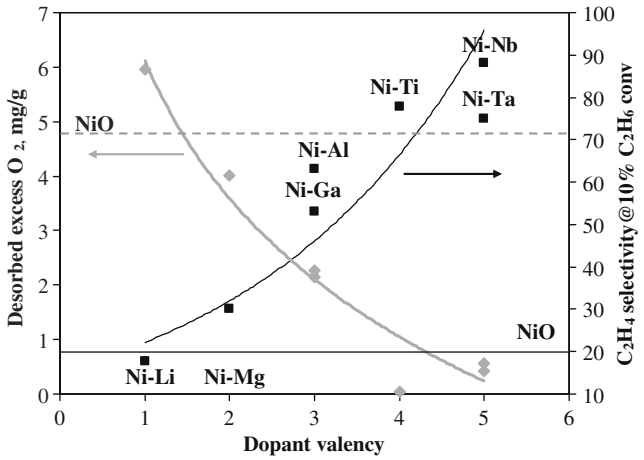

Fig. 10. Ethene selectivity at 10% ethane conversion and amount of desorbed oxygen in TPD-O_2 experiments as a function of metal Me valence in Ni–Me–O catalysts.

The previous observations reinforce and generalize the conclusions previously drawn on the Ni–Nb–O system. NiO is a non-stoichiometric oxide with cationic vacancies which induce the formation of p^+ holes, in the form of O^- ions, to maintain charge neutrality conditions. These oxygen species are electrophilic in nature and mostly responsible for the total oxidation of ethane to CO_2 on the pure NiO sample. When a foreign metal is introduced in the NiO structure and given that the ionic radius is such that the foreign cation can insert the oxide host lattice, a solid solution is formed. In the case of Ni–Li–O, the dopant's valence is lower than Ni, and the substitution process results in an extra negative charge, which induces the formation of O^- species to maintain neutrality conditions. This is in accordance with the O_2-TPD measurements which showed an increase in the amount of desorbed oxygen, the TPIE experiments that demonstrated the exchange of a large amount of oxygen at low temperatures in Li/NiO and the decreased selectivity in the ethane ODH reaction, due to the highly oxidizing electrophilic oxygen species. In the case of doping with a higher valence element, the extra positive charge induced by the substitution process reduces the surface defects and consumes or eliminates the incompletely reduced electrophilic oxygen species, thus significantly suppressing the total oxidation of ethane to CO_2 and enhancing the selective conversion to ethylene. The higher the valence of the dopant, the higher the extra positive charge in the NiO lattice, and therefore the lower the oxygen species and the higher the ethylene selectivity, as clearly demonstrated by the presented data in this work.

4. Conclusions

The present systematic study of a series of Ni-based mixed oxides with doping metals varying from low (+1) to high valence (+5) elements clearly demonstrates the large effect of the dopant in both the physicochemical properties and the catalytic behavior of Ni–Me–O mixed oxides in the ethane oxidative dehydrogenation reaction. The dopants (Li, Mg, Al, Ga, Ti, Nb) easily insert the NiO lattice and form solid solutions, independent of the valence of the foreign species and given a similar ionic radius to Ni^{2+}. This substitution process occurring upon the introduction of the foreign elements seems to be responsible for the increase or decrease in nickel oxide's non-stoichiometry. Results obtained via the temperature-programmed desorption of oxygen and temperature-programmed isotopic oxygen exchange are consistent with the principle of controlled valence and clearly confirm that the dissolution of lower/equal to nickel valence cations (Li^{1+}, Mg^{2+}) increases the non-stoichiometric oxygen in NiO, while the higher valence cations (Al^{3+}, Ga^{3+}, Ti^{4+} Nb^{5+}, Ta^{5+}) act as electron donors and reduce the positive p^+ hole concentration and consequently the electrophilic O^- radicals of the NiO acceptor. Furthermore, not only the quantity but also the lability of the oxygen species is affected by the presence of the different dopants, with high valence dopants resulting in more strongly bonded oxygen species. The linear relationship established between the surface rate of ^{16}O exchange in the TPIE experiments and the surface rate of C_2H_6 consumption in the ODH activity tests confirms that the monitored oxygen species do participate and play an active role in the mechanism of ethane activation and conversion. The clear correlation between the non-stoichiometric oxygen that catalysts accommodate and the ability to selectively convert the ethane substrate to ethylene, with these two values following an inverse trend with increasing foreign cation valence, strongly supports the above. The

higher the dopant cation's valence, the higher is the initial selectivity to the desired product, with Ni–Nb exhibiting the highest selectivity (90%) and Ni–Li the lowest (19%).

Therefore, an important outcome of this work is that the catalytic properties of NiO in ethane ODH can be tuned with doping, according to the nature of the dopant in Me-promoted NiO catalysts. Based on the valence of the foreign species, the dopants can increase or decrease the unselective electrophilic oxygen radicals of NiO, leading to, respectively, reduced or enhanced activity in the selective conversion of ethane to ethylene.

Acknowledgments

These results have been achieved within the framework of the 1st call on Applied Catalysis carried out by ACENET, with funding from the General Secretariat for Research and Technology (GSRT), Greece. The authors sincerely thank Mr. Dimitris Sfakianakis and Ms. Zinovia Skoufa for their valuable help with the experimental work presented in this work.

References

[1] M. Eramo, Oil Gas J. 103 (45) (2005) 52.
[2] A.H. Tullo, Chem. Eng. News 79 (12) (2001) 18.
[3] G. Centi, F. Cavani, F. Trifiro, Selective Oxidation by Heterogeneous Catalysis, Kluwer Academic Publishers/Plenum Press, New York, 2001.
[4] M.A. Banares, Catal. Today 5 (1999) 319.
[5] H.X. Dai, C.T. Au, Curr. Top. Catal. 3 (2002) 33.
[6] H.H. Kung, Adv. Catal. 40 (1994) 1.
[7] V.C. Corberan, Catal. Today 99 (2005) 33.
[8] P. Botella, E. Garcia-Gonzalez, A. Dejoz, J.M. Lopez Nieto, M.I. Vazquez, J. Gonzalez-Calbet, J. Catal. 225 (2004) 428.
[9] L. Leveles, K. Seshan, J.A. Lercher, L. Lefferts, J. Catal. 218 (2003) 296.
[10] L. Leveles, K. Seshan, J.A. Lercher, L. Lefferts, J. Catal. 218 (2003) 307.
[11] E. Heracleous, A.F. Lee, I.A. Vasalos, A.A. Lemonidou, Catal. Lett. 88 (2003) 47.
[12] E. Heracleous, M. Machli, A.A. Lemonidou, I.A. Vasalos, J. Mol. Catal. A 232 (2005) 29.
[13] E. Heracleous, A.F. Lee, K. Wilson, A.A. Lemonidou, J. Catal. 231 (2005) 159.
[14] E. Heracleous, A.A. Lemonidou, J. Catal. 237 (2006) 162.
[15] E. Heracleous, A.A. Lemonidou, J. Catal. 237 (2006) 175.
[16] Y. Schuurman, V. Ducarme, T. Chen, W. Li, C. Mirodatos, G.A. Martin, Appl. Catal. A 163 (1997) 227.
[17] X. Zhang, Y. Gong, G. Yu, Y. Xie, J. Mol. Catal. A 180 (2002) 293.
[18] X. Zhang, J. Liu, Y. Jing, Y. Xie, Appl. Catal. A 240 (2003) 143.
[19] Y. Liu, US Patent 6 436 871 and 6 417 422, to Symyx Technologies, 2002.
[20] B. Solsona, F. Ivars, A. Dejoz, P. Concepción, M.I. Vázquez, J.M. López Nieto, Top. Catal. 52 (2009) 751.
[21] F. Cavani, N. Ballarini, A. Cericola, Catal. Today 127 (2007) 113.
[22] E. Heracleous, A. Delimitis, L. Nalbandian, A.A. Lemonidou, Appl. Catal. A 325 (2007) 220.
[23] J. Wang, L. Dong, Y. Hu, G. Zheng, Z. Hu, Y. Chen, J. Solid State Chem. 157 (2001) 274.
[24] J.S. Choi, H.H. Kwon, T.H. Lim, S.A. Hong, H.I. Lee, Catal. Today 93–95 (2004) 553.
[25] J.T. Richardson, B. Turk, M.V. Twigg, Appl. Catal. A 148 (1996) 97.
[26] A. Bielanski, R. Dzeinbaj, J. Slozynski, Bull. Acad. Pol. Sci. 14 (1966) 569.
[27] M.E. Dry, F. Stone, Discuss. Faraday Soc. 58 (1959) 192.
[28] M. Atanasov, D. Reinen, J. Electron. Spectrosc. Relat. Phenom. 86 (1997) 185.
[29] E. Antolini, Mater. Chem. Phys. 82 (2003) 937.
[30] G.A. El-Shobaky, N.Sh. Petro, Surf. Technol. 9 (1979) 415.
[31] J.S. Choi, H.Y. Lee, K.H. Kim, J. Phys. Chem. 77 (20) (1973) 2430.
[32] P.A. Cox, Transition Metal Oxides: An Introduction to their Electronic Structure and Properties, Oxford University Inc., New York, 1992. pp. 170–178.
[33] G.K. Boreskov, Discuss. Faraday Soc. 41 (1966) 263.
[34] E.R.S. Winter, J. Chem. Soc. 12 (1968) 2889.
[35] T. Chen, W. Li, C. Yu, R. Jin, H. Xu, Stud. Surf. Sci. Catal. 130 (2000) 1847.